analytical chemistry

ARTICLE

pubs.acs.org/ac

Highly Sensitive Electrochemiluminescence Detection of Single-Nucleotide Polymorphisms Based on Isothermal Cycle-Assisted Triple-Stem Probe with Dual-Nanoparticle Label

Hong Zhou, Jing Liu, Jing-Juan Xu,* and Hong-Yuan Chen

Key Laboratory of Analytical Chemistry for Life Science, School of Chemistry and Chemical Engineering, Nanjing University, Nanjing 210093, China

ABSTRACT: We report here a new electrochemiluminescence (ECL) approach for detection of single nucleotide polymorphisms (SNPs) based on isothermal cycle-assisted triple-stem probe labeled with Au nanoparticles (NPs) and CdTe NPs. The system is composed of a CdS nanocrystals (NCs) film on glassy carbon electrode (GCE) as ECL emitter attached a double-stem DNA probe labeled with Au NPs. Then, the third stem labeled with CdTe NPs hybridizes with the double-stem DNA to form a triple-stem probe with the two labels near the CdS NCs film. A dual-quenched ECL of CdS NCs film is achieved due to energy transfer (ET) from CdS NCs to Au NPs and CdTe NPs, which makes the sensor exhibit relatively low background. Once the one base mutant DNA (mDNA) sequence as target of SNPs analysis displaces the third stem and hybridizes with the double-stem probe, forcing Au NPs away from the CdS NCs film, an ECL enhancement by the ECL-induced surface plasmon resonance of Au NPs is observed. Furthermore, after an isothermal cycle induced by primer, polymerase, and nicking endonuclease (NEase), a further enhancement of ECL is obtained. Taking advantages of the isothermal circular amplification system and the triple-stem probe architecture which enables turning its high selectivity toward specific target sequences, the reported biosensor shows excellent discrimination capabilities of SNPs with high selectivity and low detection limit (35 aM).

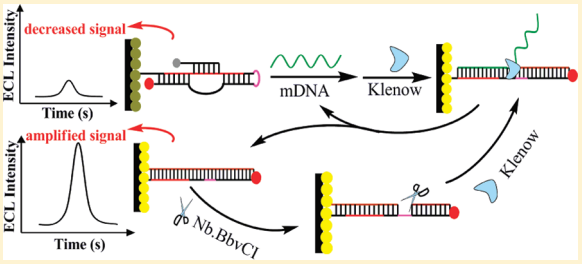

The most common form of genetic variation in human genes is single-nucleotide polymorphism (SNP),[1,2] which is a single-base variation in genome and closely associated with susceptibility to various common diseases such as diabetes, obesity, hypertension, Alzheimer's disease, cancer, etc.[3,4] Accurate and sensitive methods for SNPs analysis is essential in DNA diagnostics. Single-stem molecular beacon and double-stem pseudoknot were widely employed in electrochemical sensors to identify target DNA.[5−7] Though single-stem molecular beacon and double-stem pseudoknot based electrochemical sensors had many advantages, they also showed insufficiency in effective applications with high sensitivity which was essential for biosensors. For point of development of DNA biosensor with very high sensitivity and the ability to discriminate closely related sequences, Xiao et al. recently opened a new horizon for highly selective detection of biomarkers using a triple-stem DNA probe.[8,9] The triple-stem DNA probe which consisted of three segments of complementary duplex DNA showed its remarkable capability of specific discrimination. They found that the exceptional specificity of the triple-stem probe originated from its distinctive thermodynamic stability. At room temperature, the discontinuous duplex in the probe was less stable than the continuous perfectly matched target−probe duplex. Therefore, the presence of the perfectly matched target disrupted the native probe structure efficiently, which resulted in target−probe hybridization. In contrast, the native triple-stem structure was markedly more stable than duplexes containing a single mismatch and therefore inhibited one-base mismatched target−probe hybridization. The triple-stem probe based electrochemical SNP sensor exhibited superior mismatch discrimination at room temperature compared to single-stem molecular beacon and double-stem pseudoknot based electrochemical sensors. Nevertheless, the sensitivity of a triple-stem probe assisted SNP sensor seemed to be no better than single-stem molecular beacon and double-stem pseudoknot assisted electrochemical sensors due to the distinctive thermodynamic properties that were inherent in its structure. In order to improve the sensitivity of the biosensor, some signal amplification approaches such as polymerase chain reaction (PCR),[10,11] rolling circle amplification (RCA),[12,13] and ligases[14] have been used. However, they still have many limitations, such as being time-consuming and having contamination and high cost. Therefore, the isothermal amplification reactions based on DNA machines attracted our attention to design the sensitive analysis of SNPs for their autonomous circular amplification and simple operations. For example, Willner et al. used enzyme-assisted replication or scission reactions as the DNA machines to perform a mechanical operation and synthesize a peroxidase-mimicking DNAzyme, which, in turn, generates

Received: August 26, 2011
Accepted: September 16, 2011
Published: September 16, 2011

colorimetric or chemiluminescence readout signals, and then realized the amplified detection of DNA,[15−17] small molecules,[18] and metal ions.[19] Compared with other sensitive approaches known so far, DNA machines can perform circular amplification autonomously and effectively only under simple and easy operations. For these merits, the DNA machines may have more important future applications.

Among the diverse DNA detection techniques, the electrochemiluminescence (ECL) technique, offering a lot of advantages such as low cost, wide range of analytes, low background signal, and high sensitivity, has also been extensively used for biosensing.[20−22] Semiconductor NC, since its first use for the ECL sensor proposed in 2004, has showed its extraordinary performance in the design of ECL bisensor.[23] Subsequently, CdS, CdSe, and CdTe NCs have become the popular ECL emitters of NCs in aqueous systems.[24−33] Most of them were based on controlling the formation of excited states through changing the electron transfer processes between electrogenerated species before ECL emission. Recently, the energy transfer systems between semiconductor NCs film and nanoparticles or $Ru(bpy)_3^{2+}$ were designed in our group.[34−38] For example, we have found that the efficient electrochemiluminescence (ECL) quenching was achieved by CdTe nanoparticles through ECL energy scavenging. We also found that ECL emission from NCs film could induce surface plasmon resonances (SPR) of Au nanoparticles (NPs) and the induced SPR in turn enhance the ECL response of NCs.

In this study, we report an efficient method to fabricate the ECL sensor combining the double-nanoparticle labeled triple-stem probe and isothermal cycle technique to make sensitive and specific detection of mutant DNA (mDNA). The dual-quenched ECL of CdS nanocrystals (NCs) film, achieved by energy transfer (ET) via Au NPs and CdTe NPs, largely lowered the initial signal. Then, the continuous perfectly matched mDNA disrupted the triple-stem structure and displaced the CdTe labeled probe, resulting in an enhancement of ECL. Furthermore, after isothermal cycle induced by primer, polymerase, and nicking endonuclease (NEase), a further enhancement of ECL was obtained because the conformational changed probe as a "DNA machine" was activated and yielded a large amount of DNA triggers which could activate subsequent triple-stem probes to initiate additional replication and scission. The reported biosensor shows excellent discrimination capabilities of SNPs with high specificity and low detection limit (35 aM).

EXPERIMENTAL SECTION

Reagents. Labeled DNA oligonucleotides were ordered from Shenggong Bioengineering Ltd. (Shanghai, China), and their sequences were listed in Table 1.

Tellurium powder (99.99%), $CdCl_2 \cdot 2.5H_2O$ (99.0%), and $NaBH_4$ (96%) were obtained from Tianjin Chemical Reagent Plant (Tianjin, China). Bovine serum albumin (BSA), imidazole, 3-mercaptopropionic acid (MPA), *N*-(3-dimethylaminopropyl)-*N*′-ethyl-carbodiimide hydrochloride (EDC), *N*-hydroxysuccinimide (NHS), and tri(2-carboxyethyl) phosphine hydrochloride (TCEP) were obtained from Sigma-Aldrich (St. Louis, MO) and used without further purification. NEB buffer 2 solution and Nb.BbvCI nicking endonuclease were from New England Biolabs, Inc. The deoxynucleotide solution mixture (dNTPs) and polymerase Klenow fragment exo_ were purchased from TaKaRa Bio Inc. (Dalian, China). Phosphate buffer solution (0.1 M; KH_2PO_4−K_2HPO_4−NaCl; PBS) containing 0.05 M $K_2S_2O_8$ (pH 8.3) as a coreactant was used for ECL detection. Tris−HCl buffer (50 mM; pH 7.9) containing 50 mM NaCl and 12.5 mM $MgCl_2$ was used for DNA hybridization, while 0.1 M NaCl−Tris−HCl buffer (pH 7.4) and 0.1 M Tris−HCl buffer (pH 7.4) were employed for assembly or rinse of electrode. All other reagents were of analytical grade and used as received. Millipore ultrapure water (resistivity ≥ 18.2 MΩcm) was used throughout the experiment.

Table 1. DNA Sequence Used in This Work

Name	Sequences (5' to 3')
Duple–stem DNA Probe[a]	NH_2- TTT TTT ACT TGG ACC **GGG CAG CAC** GAA TGG *CCT CAG C*GC CAT TTA TTT TTT TTT AGG TCC AAG T-SH
DNA Probe[b]	**C GTG CTG CCC** TTT TTT-NH_2
Mutant DNA (mDNA)[c]	G CCA TTC GTG CT[G] CCC GGT CCA AGT
Wild-type DNA	GC CAT TCG TGC T[T]C CCG GTC CAA GT
bio-bar-code DNA (bbcDNA)	SH-GCG CGA ACC GTA TA
Primer	ACT TGG AC

[a] The underlined region identifies the complementary sequence to the primer. The NEase recognition site of the target is the italicized region. [b] The blue portion is complementary with the mutant DNA (mDNA), and the boldface is complementary with the boldface of DNA Probe. [c] The mutant base is highlighted in the box.

Apparatus. The electrochemical and ECL emission measurements were conducted on a MPI-A multifunctional electrochemical and chemiluminescent analytical system (Xi'An Remax Electronic Science &Technology Co. Ltd., Xi'An, China) at room temperature. The spectral width of the photomultiplier tube (PMT) was 350−650 nm, and the voltage of the PMT was set at 500 V in the process of detection. The experiments were carried out with a conventional three-electrode system. The working electrode was a 3 mm diameter glassy carbon electrode (GCE) modified with NCs composite film, meanwhile, a Pt wire and SCE electrode served as the counter and reference electrodes, respectively. Transmission electron microscopy was performed with a JEOL model 2000 instrument operating at 200 kV accelerating voltage. The UV−vis absorption spectra were obtained on a Shimadzu UV-3600 UV−vis-NIR photospectrometer (Shimadzu Co.).

Synthesis of CdS NCs. CdS NCs were prepared according to the literature.[38] Briefly, $Cd(NO_3)_2 \cdot 4H_2O$ (0.1683 g) was dissolved in 30 mL of ultrapure water and heated to 70 °C under stirring; then, a freshly prepared solution of Na_2S (0.5960 g) in 30 mL of ultrapure water was slowly injected, and instantly, an orange-yellow solution was obtained. The reaction was held at 70 °C for 3 h with continuous refluxing. The final reaction precipitates were centrifugated and washed thoroughly with absolute ethanol two times and ultrapure water two times. Then, the obtained precipitate was redispersed into water for centrifugation to collect the upper yellow solution of CdS NCs. The final solution was stored at 4 °C when not in use.

Preparation of Au Nanoparticles (Au NPs). Au NPs were prepared by sodium borohydride reduction of $HAuCl_4$ according to the methods reported previously with a slight modification.[39,40] All glassware was cleaned with chromate washings (cleaning solution), rinsed with water, and oven-dried prior to use. Ice cold 0.1 M $NaBH_4$ (600 μL) was added to 20 mL of aqueous solution

containing 2.5×10^{-4} M $HAuCl_4$ under stirring. The mixture immediately turned to orange-red color, indicating the formation of gold nanoparticles. Keep on stirring in an ice bath for 10 min. Then, the solution reacted at room temperature with continuous stirring for another 3 h until the color changed from orange-red to wine red. The prepared colloid Au NPs were stored in brown glass bottles at 4 °C for further use.

Preparation of Biobar-Code DNA/Double-Stem DNA Probe/Au NPs Composite (bbc-ds-DNA-Au NPs). The bbc-ds-DNA-Au NPs were prepared according to the reference with a slight modification.[41] Briefly, 50 μL of 1 μM double−stem DNA and 4 μM biobar-code DNA (noncomplementary to mDNA) in 0.1 M NaCl + 0.1 M Tris−HCl buffer (pH 7.4) were activated with 1.5 μL of 10 mM TCEP before use, in order to reduce disulfide bonds, and then, 500 μL of Au colloidal solution containing 0.5 mM $MgCl_2$ was added into the mixture. The double-stem DNA was complementary to mDNA, and bbcDNA was non-complementary. The low density of double-stem DNA on Au NPs would be favorable to the one-to-one combination of mDNA; compared with single DNA probe strands, Au NPs containing dsDNA and bbcDNA could avoid cross-reaction and improve the detection sensitivity of mDNA. The resulting colloidal solution was kept in refrigerated at 4 °C for 24 h. Finally, the resulting bbc-ds-DNA-Au NPs were washed three times with 0.1 M Tris−HCl buffer and resuspended in solution and stored at 4 °C for further use. The bbc-ds-DNA-Au NPs conjugates were denoted probe 1.

Synthesis of CdTe NPs. CdTe NPs were synthesized as in the literature with some modification.[42] Briefly, 0.069 g of $CdCl_2 \cdot 2.5H_2O$ was dissolved in 25 mL of water, and 55 μL of MPA was added followed by deaeration with N_2 for 30 min. Next, oxygen-free NaHTe solution, which was freshly prepared from 0.016 g of tellurium powder and 0.3 g of $NaBH_4$ in 25 mL of water at 60 °C, was injected into the above solution under vigorous stirring. Herein, the molar ratio of Cd^{2+}/MPA/HTe was fixed at 1:2:0.41. The solution was then refluxed at 100 °C for 3 h. The final reaction mixture was purified by centrifugation in absolute ethanol and dried in a vacuum. For the activation of carboxylic acid group on the surface of CdTe NPs, 1.0 mg of CdTe NPs was dispersed in 1 mL of 0.1 M imidazole−HCl buffer (pH 7.0) containing 25 mg of EDC and 12 mg of NHS and activated for 1.5 h at room temperature. The activated CdTe NPs were separated by centrifugation and washed with water and 0.01 M PBS buffer (pH 7.4) alternatively for several times followed by redispersion in 1 mL of 0.01 M PBS buffer (pH 7.4).

Preparation of CdTe/DNA Conjugates. CdTe NPs (100 μL of 1 $mg \cdot mL^{-1}$) in 0.01 M PBS (pH 7.4) was mixed with 150 μL, 1 μM DNA, followed by incubation at 25 °C for 12 h. For the blocking of nonspecific binding sites of CdTe NPs, 100 μL of 2 wt % BSA was added into the CdTe-DNA conjugates solution and incubated at 25 °C for another 2 h. The resulting conjugates were separated by centrifugation and redispersed in 300 μL of 0.01 M PBS buffer (pH 7.4). The CdTe-DNA-BSA conjugates were denoted probe 2.

Preparation of CdS NCs Film. The GCE was polished in sequential order with 1.0, 0.3, and 0.05 μm of alumina. Then, the GCE was thoroughly rinsed with water, sonicated in ethanol and ultrapure water in turn, and finally dried in air. The CdS NCs film was achieved by dropping 10 μL of CdS NCs solution onto the pretreated surface of GCE and evaporated in air at room temperature. At last, the CdS NCs modified GCE was stored in 0.1 M NaCl + 0.1 M Tris−HCl buffer (pH 7.4) for characterization and further modification.

Preparation of ECL Biosensor. The CdS NCs modified GCE was immersed in 1.0 mL of 0.1 M NaCl + 0.1 M Tris−HCl buffer (pH 7.4) containing 3 mM MPA for 6 h at 25 °C for assembly of MPA. After rinsing thoroughly with water and Tris−HCl buffer, the terminal carboxylic acid groups of the MPA/CdS/GCE were activated by immersion in 1.0 mL of 0.1 M imidazole−HCl buffer (pH 7.0) containing 20 mg of EDC and 10 mg of NHS for 1 h at room temperature. Then, the electrode was rinsed with 0.1 M Tris−HCl buffer (pH 7.4) to wash off the excess EDC and NHS. Finally, the resulting linker/MPA/CdS/GCE was soaked in the stable colloidal solution of bbc-ds-DNA-Au NPs composites (100 μL) for 24 h at 25 °C. Subsequently, 2 wt % BSA solution was used at 25 °C for 1 h for the purpose of blocking the nonspecific active binding sites of the CdS NCs. Finally, the electrode was soaked in 100 μL of CdTe-DNA-BSA conjugates (probe 2) and hybridized to form the triple-stem probe. The electrode surface was rinsed with 0.1 M NaCl−Tris−HCl buffer (pH 7.4) after each step to remove nonspecifically adsorbed species.

Amplifield ECL Detection of mDNA. The resulting electrode was immerged in a 100 μL solution consisting of 50 mM NaCl, 12.5 mM $MgCl_2$, 0.1 mM dithiothreitol, 50 mM Tris−HCl (pH 7.9), 1.25 mM dNTPs, 5.0×10^{-8} M primer, 0.1 U μL^{-1} polymerase Klenow fragment exo_, and 0.2 U μL^{-1} Nb.BbvCI nicking endonuclease in 0.1% Triton X100. A series of mDNA at different concentrations were then added to the mixture solution, and then, the mixture was incubated at 25 °C for 60 min. Subsequently, the electrode was washed thoroughly with the 0.1 M NaCl−Tris−HCl buffer (pH 7.4) to remove unhybridized oligonucleotide followed by the measurement of ECL. ECL detection was accomplished with the electrodes in 0.1 M PBS (pH 8.3) containing 0.05 M $K_2S_2O_8$ and the potential range of 0 to −1.4 V. The voltage of the PMT was set at 500 V in the process of detection. ECL signals related to the mDNA concentrations could be measured. The data of three independent measurements were presented with an error margin of one standard deviation.

Nondenaturing Polyacrylamide Gel Electrophoresis. The triple-stem DNA probe and the products by the DNA machine's isothermal strand-displacement polymerization reaction were characterized by 20% native polyacrylamide gel electrophoresis (Acr = acrylamide, Bis = *N*,*N*′-methylenebisacrylamide; Acr/Bis = 19/1). Tris−acetate−EDTA (TAE) (pH = 8.3) was used as the separation buffer. Electrophoresis was carried out at 120 V for 1.5 h at 25 °C. The visualization and photography were performed using a digital camera under UV illumination.

RESULTS AND DISCUSSION

Preparation of the Triple-Stem Probe and the Reaction Mechanism. The triple-stem probe consisted of two single-strand DNA probes (a double-stem DNA/Au NPs probe 1 and a DNA/CdTe NPs probe 2, Scheme 1A). At room temperature, the probe 1 self-hybridized into two separate stems ($\triangle G$ = −14.34 kcal/mol) and then hybridized with probe 2 ($\triangle G$ = −22.88 kcal/mol) to form three separate stems which was expected to be a discontinuous, 25 base double helix. In the presence of perfectly matched mDNA, the triple-stem probe conformational changed and the probe 2 was displaced, owing to being entropy driven. The free energy change decreased in this process. The free energy difference between the complex of probe and mutant DNA which was 25 base hybridization ($\triangle G$ = −55.54 kcal/mol)

Scheme 1. (A) Preparation of Triple-Stem DNA Probe. (B) Schematic Representation of Nanomaterial and Isothermal Circular-Assisted Triple-Stem DNA Probe Assisted ECL Signal Amplification for Amplified Assay of mDNA

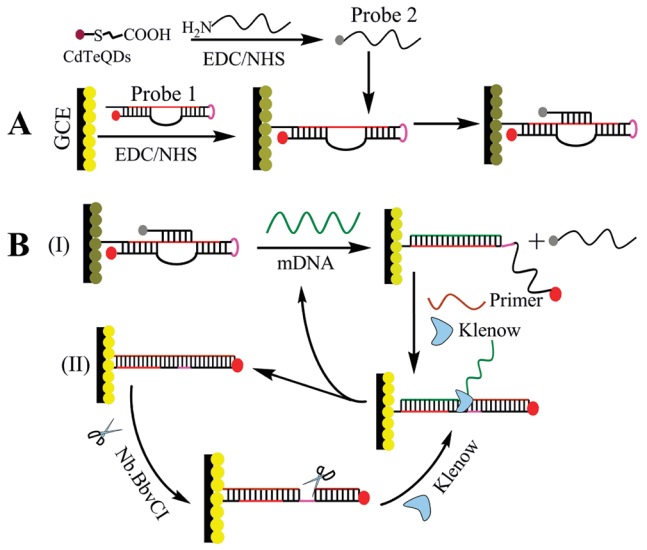

was approximately estimated according to the Integrated DNA Technologies (http://www.idtdna.com/analyzer/Applications/OligoAnalyzer/Default.aspx) with DNA parameters for 25 °C and salt conditions being 50 mM Na^+ and 12.5 mM Mg^{2+}. Such a forward reaction automatically occurred due to $\triangle G < 0$.[43]

Principle of the Amplified mDNA Detection Method. The designed ECL-SNP sensor based on isothermal cycle assisted ECL signal amplification contained a triple-stem DNA probe (Scheme 1B, (I)) and a "DNA machine" (Scheme 1B, (II)) which consisted of a CdS NCs modified GCE, two single-strand DNA probes (a double-stem DNA/Au NPs probe 1 and a DNA/CdTe NPs probe 2), a short primer, Polymerase, and NEase. In the above biosensor, CdS NCs and CdTe NPs acted as the ECL luminophores and ECL quencher, respectively, while Au NPs were employed as both ECL quencher and enhancer. At room temperature, probe 1 self-hybridized into two separate stems, and then, it hybridized with probe 2 to form a discontinuous, 25 base double helix with three separate stems (Scheme 1A). This triple-stem probe architecture enabled turning its high selectivity toward specific target sequences. Upon hybridization with a perfectly matched mDNA sequence, the triple-stem structure was disrupted, owing to being entropy driven.[44] Herein, the mDNA replaced probe 2 labeled with CdTe NPs (ECL quencher) and bound to the complementary sequence, resulting in ECL enhancement. Meanwhile, a single-stranded DNA at the 3′ end of the probe 1 was presented to an engaging primer which initiated DNA polymerization on the probe 1 and caused it to be a more rigid, rod-like double helix. Therefore, a further enhancement of ECL occurred, owing to energy transfer of ECL induced surface plasmon resonances (SPR) of Au NPs to the CdS NCs film at large separation.[45] As such, the probe 1 acted as a template of polymerization reaction, the Au NPs carrier, and a "track" on which the machine operated and the mDNA acted as a trigger of polymerization reaction. The principle of this ECL-SNP detection system was based on the conformational change of the triple-stem probe induced by hybridization between probe and mDNA. In the polymerization reaction, the mDNA was displaced in the process of synthesis of the duplex DNA with the polymerase and then hybridized to another triple-stem probe. As a result, when the mDNA acting as DNA trigger was regenerated, another probe was "activated" and a double-stranded DNA (dsDNA) was formed during each cycle; this designed triple-stem probe allowed circular hybridization, polymerization reaction, and displacement.

In our detection system, the NEase was specifically designed to recognize specific nucleotide sequences in double-stranded DNA and cleave only one of the two strands. The middle region of the probe 1 contained the recognition sequence (−CCTCA^GC−) of a NEase, which was expected to traverse the loop region of the probe 1 (Scheme 1, pink highlight). In the absence of a DNA trigger, the triple-stem probe was "inactive" and would not yield a double strand that reacted with the NEase. Upon hybridization with mDNA (DNA trigger), in the presence of polymerase and the deoxynucleotide triphosphate (dNTPs), a dsDNA was produced and the DNA recognition sequence became a suitable substrate for the endonuclease to cleave the replicated single strand at the marked position. The cleavage of the single strand generated a new site for the initiation of following replication. Thus, the subsequent replication resulted in strand displacement and autonomously formed a large amount of DNA trigger as the machine's product. During each synthesis cycle, a DNA trigger was synthesized which can activate subsequent probes to initiate additional polymerization reactions. Once initiated, the nick, polymerization, and displacement reactions continuously cycle to produce the large amount of DNA triggers that "activate" the triple-stem probe in a cyclic chain reaction, resulting in evident increasement in ECL signal.

Characterization of the Biobar-Code DNA/Double-Stem DNA Probe/Au NPs (bbc-ds-DNA-Au NPs) Conjugates, Au NPs, CdS NCs, and CdTe NPs. The obtained bbc-ds-DNA-Au NPs conjugates could be confirmed by the UV−vis absorption spectrum. The UV−visible spectra of the Au NPs, unmodified bbc-ds-DNA, and functionalized Au NPs with bbc-ds-DNA were recorded by the spectrophotometer as shown in Figure 1A. Curve b exhibited both the characteristic absorbance of Au NPs (curve c) at ca. 520 nm and bbc-ds-DNA (curve d) at ca. 260 nm. The results indicated that the oligonucleotides had been successfully labeled on AuNPs. Figure 1B presented the typical UV−vis absorption spectrum of the CdTe NPs. The absorption spectrum indicated that the CdTe NPs had a broad absorption in the wavelength range of 350−800 nm, and the color of the CdTe NPs was black (insets in Figure 1B). Therefore, the CdTe NPs acted like black bodies to effectively absorb ECL emission.

Figure 1C,D,E showed the TEM images of Au NPs, CdS NCs, and CdTe NPs, respectively. According to the TEM observation, the average size of the Au NPs and CdS NCs was about 5 nm, and the diameter of the CdTe NPs was about 3 nm.

Mechanism of ECL Quenching and Enhancement from the CdS NCs Film by Au NPs and CdTe NPs. In our design, GCE was modified by drop-coating of 10 μL of CdS NCs and used as ECL emitters. As the electrode potential became sufficiently negative, electrons were injected into the CdS NCs immobilized on the electrode and the CdS NCs produced negatively charged radicals of $CdS^{-\bullet}$. Here, $S_2O_8^{2-}$ was added as a coreactant to produce an anion sulfate radical $SO_4^{-\bullet}$, and then, $SO_4^{-\bullet}$ could react with $CdS^{-\bullet}$ to obtain an excited state (CdS*). This state emitted light in the aqueous solution to

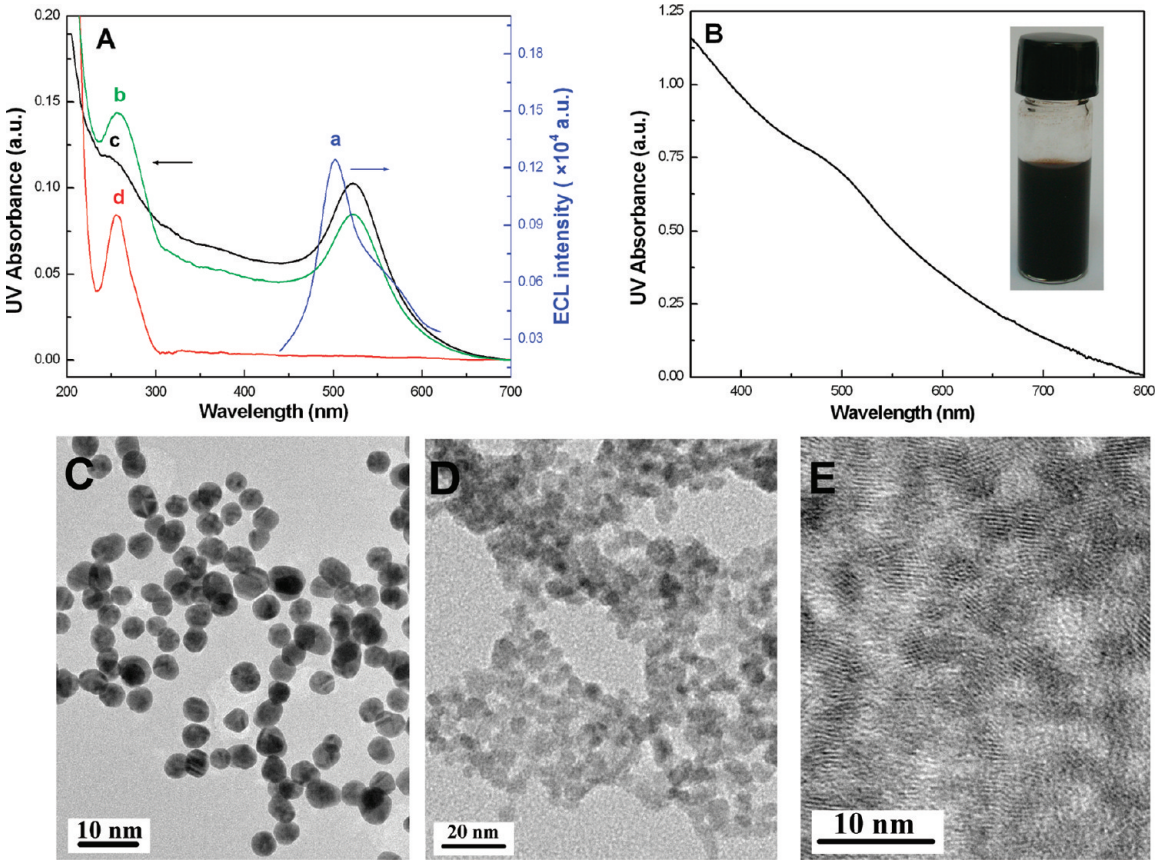

Figure 1. (A) ECL spectrum of CdS NCs film (a) and UV−vis absorption spectrum of bbc-ds-DNA-Au NPs conjugates (b), AuNPs (c), and bbc-ds-DNA (d). (B) The UV−vis absorption spectrum of CdTe NPs; inset in (B): The photographs of CdTe NPs. (C) Transmission electron microscopy (TEM) of the Au NPs, (D) TEM of the CdS NCs, and (E) TEM of the CdTe NPs.

produce an ECL signal. The ECL mechanism was listed as follows:[46,47]

$$\mathrm{CdSNCs} + ne \rightarrow n\mathrm{CdS}^{-\bullet} \quad (1)$$

$$\mathrm{S_2O_8^{2-}} + \mathrm{e^-} \rightarrow \mathrm{SO_4^{2-}} + \mathrm{SO_4^{-\bullet}} \quad (2)$$

$$\mathrm{CdS^{-\bullet}} + \mathrm{SO_4^{-\bullet}} \rightarrow \mathrm{CdS^*} + \mathrm{SO_4^{2-}} \quad (3)$$

$$\mathrm{CdS^*} \rightarrow \mathrm{CdS} + h\nu \quad (4)$$

Therefore, the CdS film generated strong and stable ECL in the presence of coreactant $S_2O_8^{2-}$ ions. In the ECL spectrum of CdS NCs film, a broad ECL emission peaked at ca. 500 nm was obtained (Figure 1A, curve a), and bbc-ds-DNA-Au NPs conjugates exhibited an absorption maximum ca. 520 nm (Figure 1A, curve b). Obviously, the ECL emission of the CdS NCs film had a considerable spectral overlap with surface plasmon absorption of Au NPs. On the basis of such overlap, which was necessary for efficient energy transfer in photoluminescence or chemiluminescence system,[48] the successful ECL energy transfer between CdS NCs and Au NPs was achieved. As for the CdTe NPs, which had a wide range of absorption and no emission, a great ECL quenching efficiency was obtained, which was largely attributed to the energy scavenging effect. Here, the CdTe NPs acted like black bodies to effectively absorb ECL emission from CdS NCs film and then dissipate it into nonradiative energy.[42]

The amplified signal of DNA hybridization associated with quenching and enhancement of ECL from the CdS NCs film by CdTe NPs and Au NPs was demonstrated in Figure 2A. The ECL peak height decreased by 42% (Figure 2A, curve b) compared with that of the CdS NCs film before assembly (Figure 2A, curve a) when the CdS NCs films as the ECL luminophores and Au NPs were at close proximity with the double-stem formation, and then, after hybridization with probe 2 to form triple-stem formation, the ECL peak height decreased by 95% (Figure 2A, curve c), indicating that the CdTe NPs efficiently absorbed ECL emission from CdS NCs films followed by nonradiative dissipation. However, upon further hybridization with mDNA, ECL intensity from CdS NCs film increased by 94% compared with that before assembly (Figure 2A, curve d). The reason was that the CdTe NPs/DNA was replaced and the energy transfer of ECL-induced surface plasmon resonances of Au NPs to the CdS NCs film occurred at large separation.[45] Subsequently, in the presence of primer, polymerase, and NEase, a further enhancement of 2-fold in ECL peak height (Figure 2A, curve e) was observed compared with that before assembly, and the ECL enhancement occurred because the conformational changed probe as a "DNA machine" was activated and yielded a large amount of DNA triggers which could activate subsequent triple-stem probes to initiate additional replication and scission. To clarify the origin of ECL signal before and after hybridization, the control experiment without the involvement of CdTe NPs and Au NPs was carried out. The results shown in Figure 2B

dx.doi.org/10.1021/ac2022629 |*Anal. Chem.* 2011, 83, 8320–8328

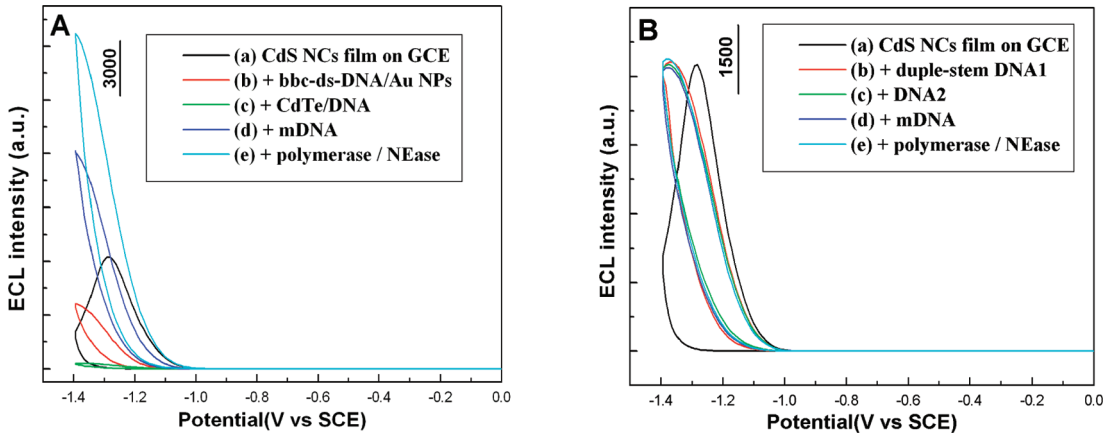

Figure 2. (A) ECL-potential curves of CdS NCs film on GCE (a); bbc-ds-DNA/Au NPs functionalized CdS NCs film on GCE (b); bbc-ds-DNA/Au NPs/CdTe NPs/DNA functionalized CdS NCs film on GCE (c); functionalized CdS NCs film on GCE in the presence of 1×10^{-7} M complementary sequence of mDNA for 1.0 h at 25 °C (d); functionalized CdS NCs film on GCE in the presence of mDNA (1×10^{-7} M), polymerse(10 U), and NEase (20U) for 1.0 h at 25 °C (e). (B) ECL-potential curves of CdS NCs film on GCE (a); double-stem DNA1 functionalized CdS NCs film on GCE (b); double-stem DNA1/DNA2 functionalized CdS NCs film on GCE (c); functionalized CdS NCs film on GCE in the presence of 1×10^{-7} M complementary sequence of mDNA for 1.0 h at 25 °C (d); functionalized CdS NCs film on GCE in the presence of mDNA (1×10^{-7} M), polymerse (10 U), and NEase (20U) for 1.0 h at 25 °C (e).

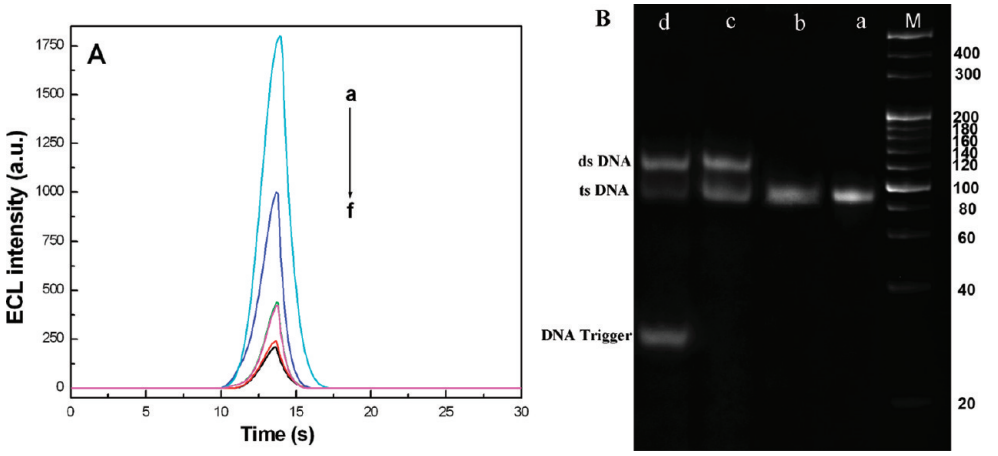

Figure 3. (A) ECL signals of sensor combined with isothermal circular system initiated with 6.0 fM mDNA in the presence of polymerase (10U) and NEase (20U) in the mixture (a), (b) was only in the presence of polymerase, (c) was only in the presence of NEase, (d) was in the absence of polymerase (10U) and NEase (20U), (e) was in the presence of polymerase (10U) and NEase (20U) but absence of mDNA in the mixture, and (f) was blank (nothing), all was reaction in the mixture at 25 °C for 60 min. (B) Nondenaturing PAGE of the isothermal circular and signal amplification system. Lanes a, b, c, and d in (B) corresponding to the results curve e, c, b, and a in (A). Experimental conditions: triple-stem DNA probe, 1×10^{-7} M; polymerase, 10 U; NEase, 20U; and mDNA, 4.0 pM.

suggested that oligonucleotide itself did not bring about any significant change in ECL intensity without the attachment of CdTe NPs and Au NPs.

Feasibility of Isothermal Circular Signal Amplification. Having proved the suitability of the ECL-SNP sensor, as designed, we now investigated the feasibility of this method for amplification of mDNA detection. As shown in Figure 3A, the ECL intensity increased obviously upon addition of target to the mixture containing both polymerase and NEase (Figure 3A, curve a), indicating that the polymerization reaction was triggered by the amplified DNA trigger as machine's product. That polymerization reaction was triggered a little even in the absence of NEase (Figure 3A, curve b) in the mixture. Nevertheless, the ECL intensity was very weak in the absence of polymerase in the mixture (Figure 3A, curve c), which was the same as in the absence of polymerase and NEase in the mixture (Figure 3A, curve d), and there was no ECL intensity change in the absence of a target (Figure 3A, curve e), indicating that no polymerization reaction was triggered, which was the same as blank (no target, polymerase, and NEase, Figure 3A, curve f). These phenomena revealed that the reaction was triggered by the product of DNA machine, implying that the detection was combined with target triggered, strand-displacement property of polymerase and NEase assisted strand-scission cycle.

The above results were further confirmed by electrophoresis. As shown in Figure 3B, lane a was only triple-stem DNA (ts DNA) probe, polymerase, and NEase but without mDNA in the mixture, which was the same as lane b with addition of ts DNA probe, mDNA, and NEase but without polymerase in the mixture. There was no new band appearance after reaction for 60 min, indicating that the primer could not open the triple-stem

dx.doi.org/10.1021/ac2022629 |*Anal. Chem.* 2011, 83, 8320–8328

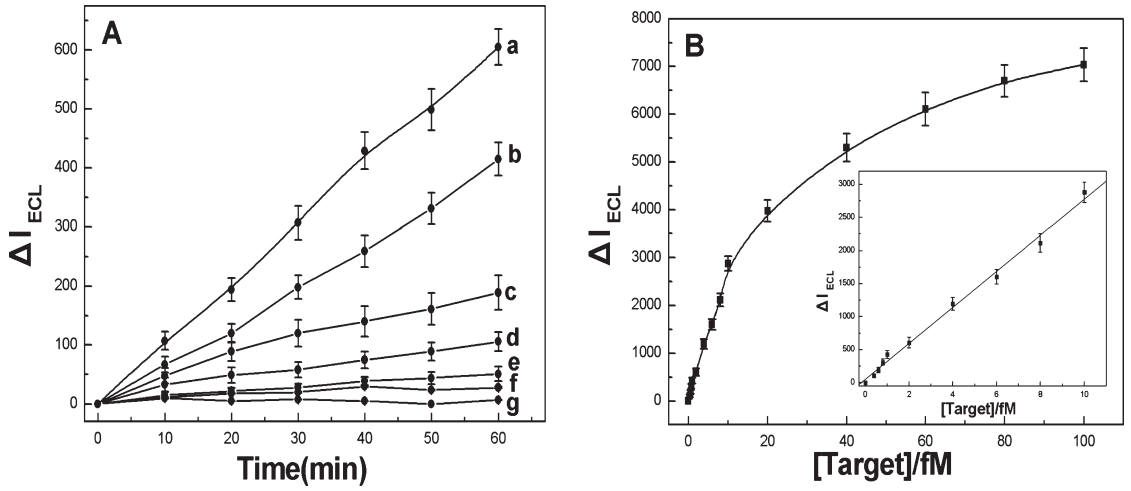

Figure 4. (A) ECL signal amplification of sensor with isothermal circular system containing polymerase and NEase and initiated with a different amount of the mDNA (a: 2 fM, b: 1 fM, c: 0.6 fM, d: 0.4 fM, e: 0.2 fM, f: 0.1 fM, g: 0). (B) Relationship between the increment in ECL peak height before and after hybridization (ΔI) and mDNA concentration after incubation at 25 °C for 60 min with isothermal circular system, three measurements for each point. Inset: calibration curve for single-base mutant target DNA.

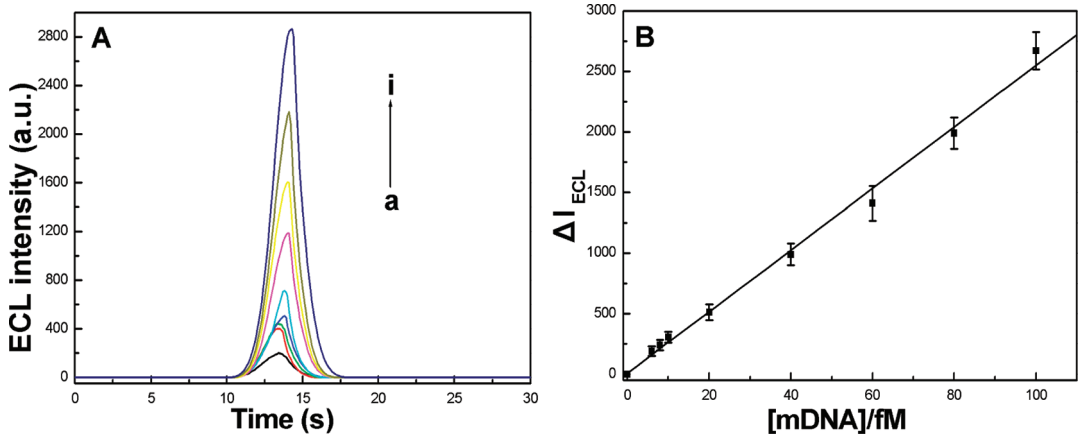

Figure 5. (A) ECL signals of the sensor incubated with different concentrations of mDNA at 25 °C for 60 min without polymerase and NEase in the mixture. (a: 0, b: 6.0×10^{-15} M, c: 8.0×10^{-15} M, d: 1.0×10^{-14} M, e: 2.0×10^{-14} M, f: 4.0×10^{-14} M, g: 6.0×10^{-14} M, h: 8.0×10^{-14} M, i: 1.0×10^{-13} M, respectively). (B) The relationship between relative ECL intensity (ΔI) and concentration of mDNA after incubation at 25 °C for 60 min without polymerase and NEase in the mixture, three measurements for each point. The concentration of mDNA was 0 M, 6.0×10^{-15} M, 8.0×10^{-15} M, 1.0×10^{-14} M, 2.0×10^{-14} M, 4.0×10^{-14} M, 6.0×10^{-14} M, 8.0×10^{-14} M, and 1.0×10^{-13} M, respectively, and the regression equation was expressed as $y = 8.9792 + 25.404$ (x was the concentration of mDNA, fM, y was ΔI, $R = 0.99725$).

probe and no polymerization reaction was triggered without mDNA or polymerase. However, after mDNA and polymerase were added in the mixture of ts DNA probe, the polymerization reaction was triggered and double-stranded DNA (ds DNA) formed with a new band observed in lane c. Lane d showed electrophoresis results of the mixture containing both polymerase and NEase with addition of mDNA. As expected, the polymerization reaction was triggered to form dsDNA probe (the first band in lane d), and the DNA trigger as machine's product appeared (the last band in lane d), revealing that the detection combined with target triggered strand-displacement property of polymerase and NEase assisted strand-scission cycle.

Amplified Detection of mDNA. The analytical performance of the designed strategy was related to the reaction time. From Figure 4A, we could find that, in the isothermal circular system containing polymerase and NEase, ECL signal increased with the increasing reaction time (0−60 min) under a different amount of the mDNA (a: 2 fM, b: 1 fM, c: 0.6 fM, d: 0.4 fM, e: 0.2 fM, f: 0.1 fM, g: 0). At 60 min, the distinction of ECL signal under a different concentration of mDNA was obvious and the ECL signal was high enough to sensitively detect mDNA. Therefore, the reaction time was selected at 60 min. The sensitivity of the ECL-SNP sensor combined with isothermal circular system was detected as shown in Figure 4B. The results showed that the relative ECL intensity ($\Delta I = I - I_0$) increased with the increase of concentration of the mDNA ranging from 0.4 fM to 100 fM for 60 min, and there was a fairly good linear relationship between the ΔI and the concentration of mDNA in the range from 0.4 fM to 10 fM (inset in Figure 4B). The regression equation was expressed as $\Delta I = 272.519C + 48.937$ (C represents the concentration of mDNA, fM; correlation coefficient $R = 0.9969$) with a limit of detection (LOD) of 35 aM mDNA (3σ), which was more

dx.doi.org/10.1021/ac2022629 |*Anal. Chem.* 2011, 83, 8320–8328

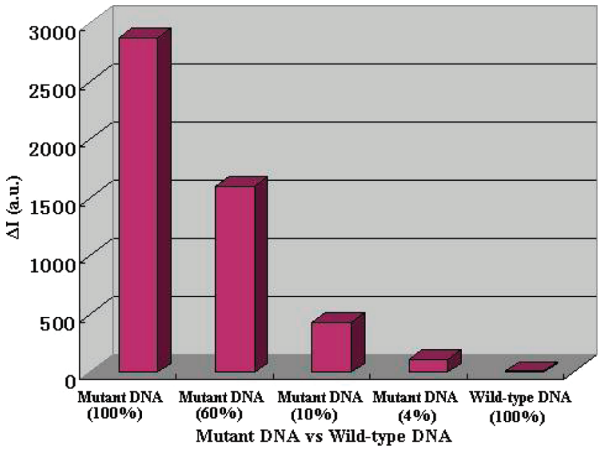

Figure 6. Effect of the mutant DNA to wild-type DNA ration on the detection of SNP. The total concentration of mutant DNA and wild-type DNA was 10 fM.

sensitive than that of the control experiment without the isothermal circular system (380 aM, Figure 5). Meanwhile, this ultrahigh sensitivity also reflected that the signal amplification of the ECL-SNP sensor combined with the isothermal cycle had been achieved.

Detection of SNP Specificity in Constructed DNA Samples. To verify the single-base specificity of this ECL-SNP sensor, the target oligonucleotides of mutated and wide-type sequences were mixed at various ratios with a total concentration of 10 fM, which subsequently reacted to the triple-stem probe with complementary sequence to the mDNA. From the results of Figure 6, the change of ECL intensity increased with the increase of mDNA percentage in the sample solution. Obviously, the ECL intensity increased substantially when only 0.4 fM mDNA existed in the mixture with the percentage of mDNA in the samples as low as 4%. The result indicated that the present approach had high specificity for detecting a trace mutation among a large quantity of wild types, which made the strategy have great potential applications in early clinical diagnosis of disease.

CONCLUSIONS

In this approach, we have developed an ultrasensitive ECL-SNP sensor that combines a triple-stem probe and a powerful isothermal amplification method with a "DNA machine", which has several combined advantages. First, a dual-quenched ECL from CdS NCs film is achieved via CdTe NPs and proximal Au NPs with triple-stem DNA probe. The sufficient quenching largely reduces the ECL signal of background. Second, the triple-stem probe architecture enables one to turn its high selectivity toward specific target sequences. Third, the isothermal circular amplification system could enhance the sensitivity of SNP detection and eliminate the requirement for thermal cycling due to the normal temperature condition. With such dramatic amplification signal and the specificity of the DNA, the concentration detection limit of 35 aM for mDNA was obtained. In conclusion, with its simplicity, selectivity, and sensitivity, this strategy as a molecular tool holds great promise for SNP discovery and analysis, and we believe it will be extensively applied in the fields of basic and clinical research and diagnostics.

AUTHOR INFORMATION

Corresponding Author
*E-mail: xujj@nju.edu.cn.

ACKNOWLEDGMENT

This work was supported by the 973 Program (2012CB932600) and the NSFC (Grant Nos. 21025522, 20975051, 21135003, 20890020) of China.

REFERENCES

(1) Altshuler, D.; Brooks, L. D.; Chakravarti, A.; Collins, F. S.; Daly, M. J.; Donnelly, P. *Nature* **2005**, *437*, 1299–1320.
(2) Wang, W.; Barratt, B. J.; Clayton, D. G.; Todd, J. A. *Nat. Rev. Genet.* **2005**, *6*, 109–118.
(3) Risch, N.; Merikangas, K. *Science* **1996**, *273*, 1516.
(4) Rapley, R.; Harbron, S. Wiley: New York, 2004.
(5) Liu, G.; Wan, Y.; Gau, V.; Zhang, J.; Wang, L. H.; Song, S. P.; Fan, C. H. *J. Am. Chem. Soc.* **2008**, *130*, 6820–6825.
(6) Cash, K. J.; Heeger, A. J.; Plaxco, K. W.; Xiao, Y. *Anal. Chem.* **2009**, *81*, 656–661.
(7) Xiao, Y.; Qu, X. G.; Plaxco, K. W.; Heeger, A. J. *J. Am. Chem. Soc.* **2007**, *129*, 11896–11897.
(8) Xiao, Y.; Plakos, K. J. I.; Lou, X. H; White, R. J.; Qian, J. R.; Plaxco, K. W.; Soh., H. T. *Angew. Chem., Int. Ed.* **2009**, *48*, 4354–4358.
(9) Xiao, Y.; Lou, X. H; Uzawa, T.; Plakos, K. J. I.; Kevin, W.; Plaxco, K. W.; Soh., H. T. *J. Am. Chem. Soc.* **2009**, *131*, 15311–15316.
(10) Ranasinghe, R. T.; Brown, T. *Chem. Commun.* **2005**, *44*, 5487.
(11) Marx, A.; Strerath, M. *Angew. Chem., Int. Ed.* **2005**, *44*, 7842.
(12) Li, J. S.; Deng, T.; Chu, X.; Yang, R. H.; Jiang, J. H.; Shen, G. L.; Yu, R. Q. *Anal. Chem.* **2010**, *82*, 2811–2816.
(13) Li, J. S.; Zhong, W. W. *Anal. Chem.* **2007**, *79*, 9030–9038.
(14) Wang, H.; Li, J. S.; Wang, Y. X.; Jin, J. Y.; Yang, R. H.; Wang, K. M.; Tan, W. H. *Anal. Chem.* **2010**, *82*, 7684–7690.
(15) Beissenhirtz, M. K.; Elnathan, R.; Weizmann, Y.; Willner, I. *Small* **2007**, *3*, 375–379.
(16) Weizmann, Y.; Beissenhirz, M. K.; Cheglakov, Z.; Nowarski, R.; Kotler, M.; Willner, I. *Angew. Chem., Int. Ed.* **2006**, *45*, 7384–7388.
(17) Zhu, C.; Wen, Y.; Li, D.; Wang, L.; Song, S.; Fan, C.; Willner, I. *Chem.—Eur. J.* **2009**, *15*, 11898–11903.
(18) Shlyahovsky, B.; Li, D.; Weizmann, Y.; Nowarski, R.; Kotler, M.; Willner, I. *J. Am. Chem. Soc.* **2007**, *129*, 3814–3815.
(19) Li, D.; Wieckowska, A.; Willner, I. *Angew. Chem., Int. Ed.* **2008**, *47*, 3927–3931.
(20) Xu, S. J.; Liu, Y.; Wang, T. H.; Li, J. H. *Anal. Chem.* **2011**, *83*, 3817–3823.
(21) Duan, R. X.; Zhou, X. M.; Xing, D. *Anal. Chem.* **2010**, *82*, 3099–3103.
(22) Xu, S. J.; Liu, Y.; Wang, T. H.; Li, J. H. *Anal. Chem.* **2011**, *82*, 9566–9572.
(23) Zou, G. Z.; Ju, H. X. *Anal. Chem.* **2004**, *76*, 6871–6876.
(24) Wang, X. F.; Zhou, Y.; Xu, J. J.; Chen, H. Y. *Adv. Funct. Mater.* **2009**, *19*, 1444–1450.
(25) Liu, X.; Zhang, Y. Y.; Lei, J. P.; Xue, Y. D.; Cheng, L. X.; Ju, H. X. *Anal. Chem.* **2010**, *82*, 7351–7356.
(26) Liu, X.; Jiang, H.; Lei, J. P.; Ju, H. X. *Anal. Chem.* **2007**, *79*, 8055–8060.
(27) Liu, X.; Ju, H. X. *Anal. Chem.* **2008**, *80*, 5377–5382.
(28) Jiang, H.; Ju, H. X. *Anal. Chem.* **2007**, *79*, 6690–6696.
(29) Cheng, L. X.; Liu, X.; Lei, J. P.; Ju, H. X. *Anal. Chem.* **2010**, *82*, 3359–3364.
(30) Zhang, L. H.; Zou, X. Q.; Ying, E. B.; Dong, S. J. *J. Phys. Chem. C* **2008**, *112*, 4451–4454.
(31) Bae, Y.; Myung, N.; Bard, A. J. *Nano Lett.* **2004**, *4*, 1153.
(32) Jie, G. F.; Zhang, J. J.; Wang, D. C.; Cheng, C.; Chen, H. Y.; Zhu, J. J. *Anal. Chem.* **2008**, *80*, 4033–4039.

(33) Jiang, H.; Ju, H. X. *Chem. Commun.* **2007**, 404–406.
(34) Shan, Y.; Xu, J. J.; Chen, H. Y. *Chem. Commun.* **2009**, 905–907.
(35) Shan, Y.; Xu, J. J.; Chen, H. Y. *Nanoscale* **2011**, *3*, 2916–2923.
(36) Wu, M. S.; Shi, H. W.; Xu, J. J.; Chen, H. Y. *Chem. Commun.* **2011**, *47*, 7752–7754.
(37) Shan, Y.; Xu, J. J.; Chen, H. Y. *Chem. Commun.* **2010**, *46*, 4187–4189.
(38) Zhou, H.; Liu, J.; Xu, J. J.; Chen, H. Y. *Chem. Commun.* **2011**, *47*, 8358–8360.
(39) Zikich, D.; Borovok, N.; Molotsky, T.; Kotlyar, A. *Bioconjugate Chem.* **2010**, *21*, 544–547.
(40) Gole, A.; Murphy, C. J. *Chem. Mater.* **2004**, *16*, 3633–3640.
(41) Hu, K. C.; Lan, D. X.; Li, X. M.; Zhang, S. S. *Anal. Chem.* **2008**, *80*, 9124–9130.
(42) Shan, Y.; Xu, J. J.; Chen, H. Y. *Chem. Commun.* **2010**, *46*, 5079–5081.
(43) Shi, C.; Zhao, C. H.; Guo, Q. J.; Ma, C. P. *Chem. Commun.* **2011**, *47*, 2895–2897.
(44) Zhang, D. Y.; Turberfield, A. J.; Yurke, B.; Winfree, E. *Science* **2007**, *318*, 1121–1125.
(45) Wang, J.; Shan, Y.; Zhao, W. W.; Xu, J. J.; Chen, H. Y. *Anal. Chem.* **2011**, *83*, 4004–4011.
(46) Myung, N.; Ding, Z. F.; Bard, A. J. *Nano Lett.* **2002**, *2*, 1315–1319.
(47) Jie, G. F.; Liu, B.; Pan, H. C.; Zhu, J. J.; Chen, H. Y. *Anal. Chem.* **2007**, *79*, 5574–5581.
(48) Huang, X.; Li, L.; Qian, H.; Dong, C.; Ren, J. *Angew. Chem., Int. Ed.* **2006**, *45*, 5140–5143.